Inorganic Chemistry
Article

Inorg. Chem. **2010**, *49*, 9875–9883 **9875**
DOI: 10.1021/ic100850f

Computational Study of Alkynes Insertion into Metal-Hydride Bonds Catalyzed by Bimetallic Complexes

Stefania Di Tommaso,[†] Vincent Tognetti,[†] Emilia Sicilia,*,[‡] Carlo Adamo,*,[†] and Nino Russo[‡]

[†] *Laboratoire d'Electrochimie, Chimie des Interfaces et Modélisation pour l'Energie, UMR CNRS 7575 ENSCP Chimie ParisTech 11, rue P. et M. Curie F-75231, Paris Cedex 05, France, and* [‡] *Dipartimento di Chimica and Centro di Calcolo ad Alte Prestazioni per Elaborazioni Parallele e Distribuite-Centro d'Eccellenza MURST, Università della Calabria, I-87030 Arcavacata di Rende, Italy*

Received April 29, 2010

Density Functional Theory investigations on the insertion mechanism of phenylacetylene into metal-hydride bonds in bimetallic (Pt,Os) catalysts have been carried out. The results obtained have been also compared with the non-reactive monometallic (Os-based) system, to elucidate the cooperative effects and to explain the observed absence of reactivity. The identified reaction path involves phenylacetylene coordination followed by the insertion into the metal-hydride bond, leading to the formation of the experimentally observed products. Both steps do not require large energies compatible with the experimental conditions. The comparison with the reaction path for the monometallic species gives some hints on the cooperative effects due to the presence of the second metal which is related to its role in the CO release for creating a coordination site for phenylacetylene and not in the insertion energetics. The calculations provide a detailed analysis of the reaction complexity and provide a rationale for the efficiency of the process.

1. Introduction

The insertion of unsaturated hydrocarbons, and more particularly of alkynes, into a metal-hydride bond is a fundamental step in many homogeneous catalytic processes[1,2] including polymerization[3] (via the Cossee mechanism),[4] hydrogenation,[5,6] and hydrosililation reactions.[7,8] A number of studies have shown that the efficiency of certain metal-based organic transformations can be improved by the participation of a second metal species. Indeed, such bimetallic synergism is widely sought in both homogeneous and heterogeneous catalytic systems.[9−15] Recently, Adams et al. reported a well-defined alkyne insertion reaction, involving osmium and ruthenium carbonyl hydride complexes, that appears to be strongly promoted by the presence of palladium or platinum phosphine groups (see Scheme 1).[16,17] They isolated and structurally characterized a bimetallic complex, $PtOs(CO)_4(SnPh_3)(PBu^t{}_3)(\mu\text{-}H)$, **1**, that appears to be an intermediate in the reaction (Scheme 1).[16] On the basis of some simple molecular orbital calculations, these authors proposed a mechanism that involves a direct interaction of the alkyne molecule with the platinum atom prior to the transfer of the hydrido ligand from the metal atoms to the alkyne. Such an approach is also adaptable to well-defined cluster complexes.[18] The choice of these transition metals (Pt and Pd) has been suggested by their tendency to accommodate electron configurations that have less than 18 electrons per metal. Indeed, an empty orbital is needed so that the alkyne could interact with

---

*To whom correspondence should be addressed. E-mail: carlo-adamo@enscp.fr (C.A.), siciliae@unical.it (E.S.).

[1] Collman, J. P.; Hegedus, L. S.; Norton, J. R.; Finke, R. G. In *Principles and Applications of Organotransitions Metal Chemistry*; University Science Books: Sausalito, CA, 1987; Chapter 10.

[2] Li, X.; Vogel, T.; Incarvito, C. D.; Crabtree, R. H. *Organometallics* **2005**, *24*, 62.

[3] Kishimoto, Y.; Eckerle, P.; Miyatake, T.; Kainosho, M.; Ono, A.; Ikariya, T.; Noyori, R. *J. Am. Chem. Soc.* **1999**, *121*, 12035.

[4] Cossee, P. J. *J. Catal.* **1964**, *3*, 80.

[5] Kluwer, A. M.; Koblenz, T. S.; Jonischkeit, T.; Woelk, K.; Elsevier, C. J. *J. Am. Chem. Soc.* **2005**, *127*, 15470.

[6] López-Serrano, J.; Lledós, A.; Duckett, S. B. *Organometallics* **2008**, *27*, 43.

[7] Dash, A. K.; Wang, J. Q.; Eisen, M. S. *Organometallics* **1999**, *18*, 4724.

[8] Takahasi, T.; Bao, F.; Gao, G.; Ogasawara, M. *Org. Lett.* **2003**, *5*, 3479.

[9] Sinfelt, J. H. *Bimetallic catalysts: discoveries, concepts, and applications*; Wiley: New York, 1983.

[10] Adams, R. D.; Captain, B. *J. Organomet. Chem.* **2004**, *689*, 4521.

[11] Yu, Z. K.; Liao, S. J.; Xu, Y.; Yang, B.; Yu, D. R. *J. Chem. Soc.* **1995**, *11*, 1155.

[12] Misumi, Y.; Ishii, Y.; Hidai, M. *J. Mol. Catal.* **1993**, *78*, 1.

[13] Naigre, R.; Chenal, T.; Cipres, I.; Dara, J. C. *J. Organomet. Chem.* **1994**, *480*, 91.

[14] Yun, H. S.; Lee, K. H.; Lee, J. S. *J. Mol. Catal A* **1995**, *95*, 11.

[15] Bianchini, C.; Giambastiani, G.; Guerrerorios, I.; Meli, A.; Oberhauser, W.; Sorace, L.; Toti, A. *Organometallics* **2007**, *26*, 5066.

[16] Adams, R. D.; Captain, B.; Zhu, L. *J. Am. Chem. Soc.* **2006**, *128*, 13672.

[17] Adams, R. D.; Captain, B.; Trufan, E.; Zhu, L. *J. Am. Chem. Soc.* **2007**, *129*, 7545.

[18] Adams, R. D.; Captain, B. *Acc. Chem. Res.* **2009**, *42*, 409.

Scheme 1

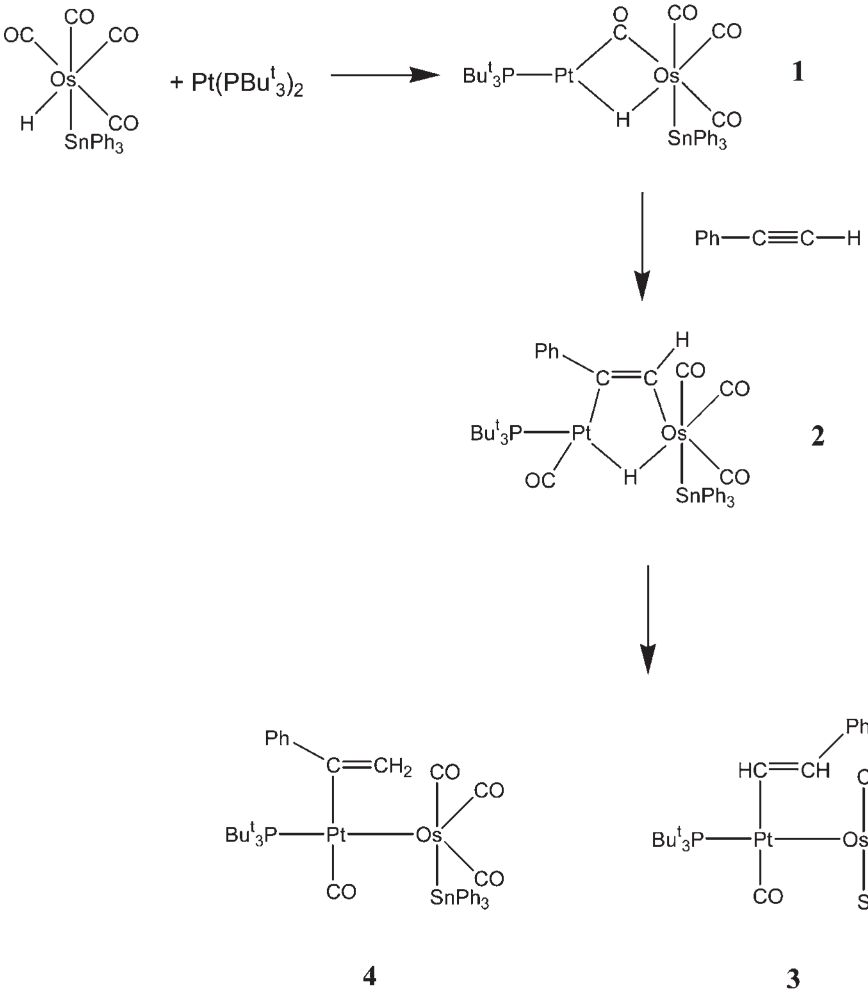

the catalyst. The results show that when phenylacetylene is added, these bimetallic precatalysts activate the metal-hydride bonds and insert the alkyne. Conversely, the one-metal parent complexes (Ru or Os alone) are unable to achieve this transformation, thus proving the essential cooperation of the metallic centers.[17]

Two challenges naturally arise from these experimental observations: the identification of the mechanism at stake in such transformations and the nature of the intermediates along the reaction path. Both deal with the process optimization and notably with the choice of the most-active metal atoms. Even if this double aim can be tackled from an experimental point of view, theory is a complementary and powerful tool to give meaningful hints about this insertion process.

Theoretical work on homogeneous bimetallic complexes has only few predecessors: the study of Bonnington et al. on platinum dimers,[19] the very recent calculations of Fragalà and Marks on Zr−Zr polymerization catalysts[20] or those of Cabeza et al.[21] on the reaction of cyclohexadiene with a hydride triruthenium complex. Besides, few other papers deal with bimetallic complexes as the simplest model for heterogeneous catalysts (see for instance reference 22 on platinum cationic clusters).

In this paper a detailed computational study of the reactions of monometallic, $HOs(CO)_4(SnPh_3)$, and bimetallic catalyst, compound **1**, with phenylacetylene, PhC_2H, are presented. In particular, all the probable reaction paths have been explored, through the energetic and structural characterization of intermediates and transition states, using an accurate computational protocol based on Density Functional Theory (DFT). Furthermore, the cooperative effects due to the presence of two metal atoms in the catalysts have been evidenced by comparing the reaction profiles obtained for the mono- and bimetallic species.

2. Computational Details

All calculations were carried out using the Gaussian 03 program[23] and the B3LYP functional (that includes 20% of Hartree−Fock exchange).[24] A two-layer ONIOM procedure[25] has been also used, in which the atoms of the first

---

(19) Bonnington, K. J.; Jennings, M. C.; Puddephatt, R. *Organometallics* **2008**, *27*, 6521.

(20) Motta, A.; Fragalà, I. L.; Marks, T. J. *J. Am. Chem. Soc.* **2009**, *131*, 3974.

(21) Cabeza, J. A.; Fernàndez-Colinas, J. M.; Pérez-Carreño, E. *Organometallics* **2009**, *28*, 4217.

(22) Xia, F.; Cao, Z. *J. Phys. Chem. A* **2006**, *110*, 10078.

(23) Frisch, M. J. et al. *Gaussian G03*, Revision B.05; Gaussian, Inc.: Wallingford, CT, 2003.

(24) (a) Becke, A. D. *J. Chem. Phys.* **1993**, *98*, 5648. (b) Stephens, P. J.; Devlin, J. F.; Chabalowski, C. F.; Frisch, M. J. *J. Phys. Chem.* **1994**, *98*, 11623.

(25) Svensson, M.; Humbel, S.; Froese, R. D. J.; Mastubara, T.; Sieber, S.; Morokuma, K. *J. Phys. Chem.* **1996**, *100*, 19357.

coordination sphere of the metals and the phenylacetylene molecule are included in the high-level part, treated at the already mentioned DFT level (see Figure 1), whereas the "low" level of theory has been described at the Hartree–Fock level. The 6-31G(d) basis set has been used for all non metallic atoms (H, C, P) belonging to the high-level part,[26] while Sn, Pt, and Os have been described using the Stuttgart-Dresden (SDD) valence basis sets in conjunction with the associated relativistic small-core effective core-potentials (ECP).[27] The LANL1 ECP and the associated minimal basis set have been used for the low-theory level in the ONIOM approach.[28]

All structures have been fully optimized, and the nature of the stationary points (minima or first-order saddle-points) has been checked by analytically computing the Hessian matrix. Moreover, intrinsic reaction coordinate (IRC) calculations[29] have been performed to verify that the products and the reactants were correctly connected.

To study the effect of medium effects on the reaction energies, the solvent (dichloromethane, as in experiments[16,17]) was described as a homogeneous isotropic dielectric medium using a polarizable continuum model, namely, the conductor-like screening model (C-PCM).[30] Enthalpies and Gibbs free energies were obtained at 298 K at 1 atm from total energies, including solvent, zero-point, and thermal corrections, using standard statistical procedures.[31] However, such approach does not reflect the real entropic cost under catalytic conditions, and the effects is particular relevant for the substrate association and dissociation.[32] Following a common approach in theoretical catalysis, the solvation entropy has been estimated as two/third of its gas-phase value.[32,33]

All species have been calculated in their singlet spin-state according to experimental data. To validate this hypothesis, the energy difference between the optimized initial bimetallic complex in the triplet and in the singlet spin-states has been computed and found to be higher than 40 kcal/mol. Views of molecular orbitals have been generated with the MOLEKEL software.[34]

3. Results and Discussion

The actual synergic action of the two metals cannot be understood and evaluated without examining the corresponding monometallic complexes. It has been underlined in reference 17 that no reaction was observed between phenylacetylene and $HOs(CO)_4SnPh_3$. This complex has been, therefore, the starting point of the investigation. The results obtained are then compared with those for the bimetallic species. In this last case, two different reaction mechanisms have been envisaged and characterized. In the first pathway the two metal atoms remain bonded as the acetylene adds to both metal atoms, while in the second pathway the two metal atoms dissociate during the acetylene addition and insertion into the metal-hydride bond. This latter path, involving dissociation and successive association of the two metallic moieties of the catalysts, is, in our opinion, highly improbable and should correspond to a reaction under entropic and diffusion control, which is not supported by experiment. Its details are given, therefore, in the Supporting Information for completeness. In a similar vein, in the Supporting Information, the validation of the computational protocol is also given, including solvent and model size effects of the catalyst and basis set choice.

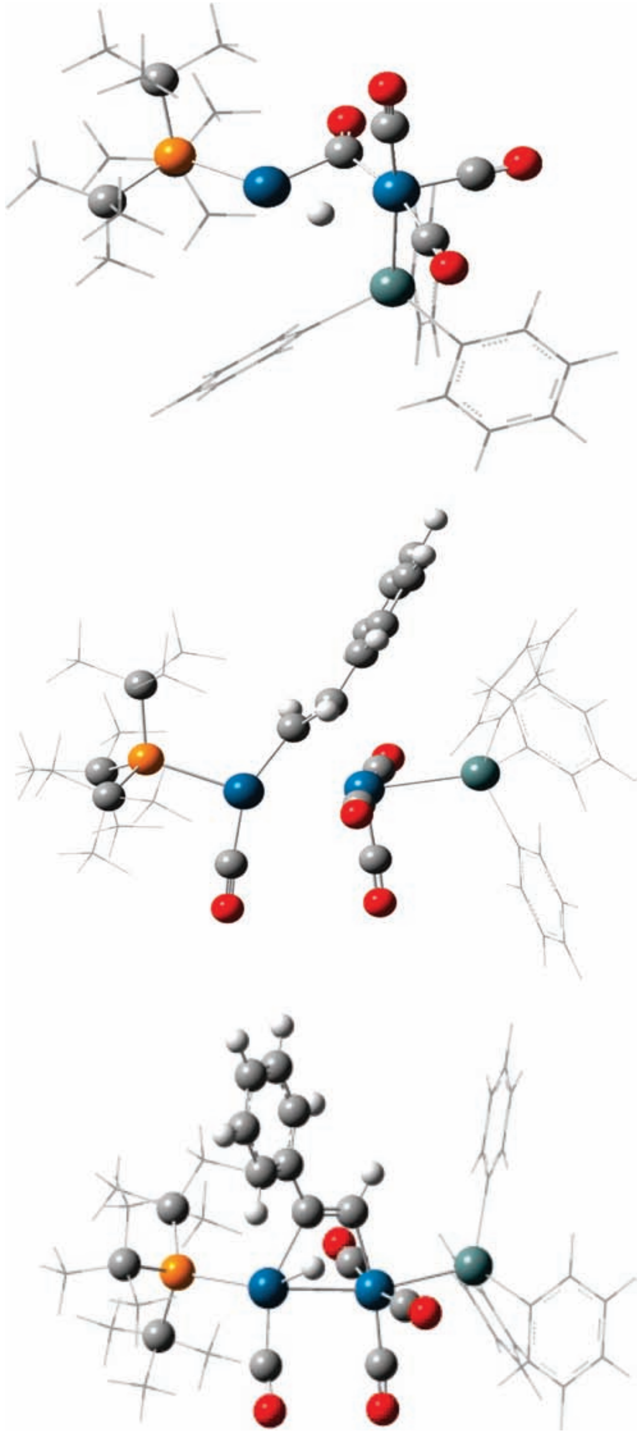

Figure 1. Views of the optimized structures of $\mathbf{1}^{\mathbf{b}}_{\mathbf{ax}}$ (up), $^{\beta}\sigma\pi_{eq}$ (middle), and $\mathbf{TS}^{\alpha}\pi\sigma_{eq}$ (down). In the ball and stick format are reported the atoms treated with the high level approach in the ONIOM model. Color code: carbon, gray; hydrogen, white; platinum and osmium, bright blue; tin, turquoise blue; oxygen, red; and phosphorus, orange.

3.1. Monometallic Paths. The simplest mechanism for the alkyne insertion catalyzed by a monometallic catalyst

---

[26] Francl, M. M.; Pietro, W. J.; Hehre, W. J.; Binkley, J. S.; Gordon, M.-H.; DeFrees, D. J.; Pople, J. A. *J. Chem. Phys.* **1982**, *77*, 3654.

[27] Dolg, M.; Wedig, U.; Stoll, H.; Preuss, H. *J. Chem. Phys.* **1987**, *86*, 866.

[28] Dunning, T. H., Jr., Hay, P. J. In *Modern Theoretical Chemistry*; Schaefer, H. F., Ed.; Plenum: New York, 1976, Vol. *3*, pp 1–28.

[29] Gonzalez, C.; Schlegel, H. B. *J. Phys. Chem.* **1990**, *94*, 5523.

[30] Tomasi, J.; Mennucci, B.; Cammi, R. *Chem. Rev.* **2005**, *105*, 2999.

[31] McQuarrie, D. A.; Simon, J. D. *Molecular thermodynamics*; University Science Books: Sausalito, CA, 1999.

[32] Cooper, J.; Ziegler, T. *Inorg. Chem.* **2002**, *41*, 6614.

[33] Tobisch, S. *Chem.—Eur. J.* **2005**, *11*, 3113.

[34] Flükiger, P.; Lüthi, H. P.; Portmann, S.; Weber, J. *Molekel 4.0*; Swiss National Supercomputing Centre CSCS: Manno, Switzerland, 2000.

Scheme 2

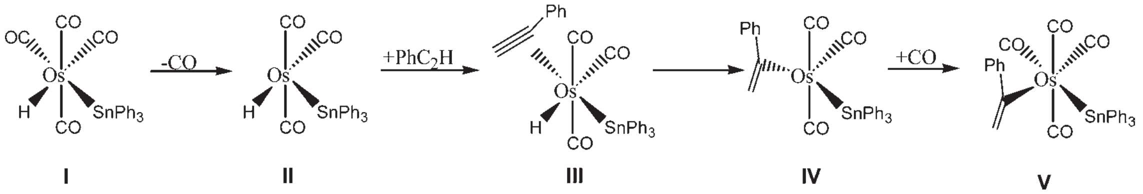

involves four steps (see Scheme 2). First, since the coordination sphere of the octahedral complex precursor **I** is saturated, a CO molecule has to be released giving **II**. Then the phenylacetylene coordinates (**III**) and inserts (**IV**). Finally, the recoordination of CO ends the process by saturating the previously created 16-electron complex (**V**). Two structural rearrangements are then possible: one where the hydride is trans to the tin group and one where it is in cis position. Then, an equatorial or an axial CO could be lost. In Figure 2 is reported the lowest energy path, corresponding to an axial CO leaving from the cis isomer; other paths, higher in energy, are reported and discussed in the Supporting Information.

The first step, which is entropy favored, requires only 13 kcal/mol while 9 kcal/mol are necessary for the second step, phenylacetylene coordination. A large overall barrier (37 kcal/mol) has to be overcome to obtain the final product, characterized by a small stabilization (less than 4 kcal/mol). Notice that it has been assumed that the elimination and the recoordination of CO occur without transition states. The most chemically striking feature of the monometallic reaction is that one CO molecule leaves the coordination sphere of metal (**II**) but another CO is necessary to have a product (**V**) more stable than the reactive. While this CO-leaving step is under thermodynamic control, the second one (CO coordination) is driven by entropy and, furthermore, strongly depends on the availability of CO in proximity of the under-coordinated metal and, therefore, on the CO diffusion in the reaction medium. In particular, the $T\Delta S$ term of this last step is 10.3 kcal/mol, about one-half of the corresponding free energy variation (23.6 kcal/mol, see Figure 2). Such a process can be therefore considered as a (very) rare event, and this fact can explain the absence of reaction experimentally observed with $\mathrm{HOs(CO)_4SnPh_3}$.[17]

Provided with these reference values the possible benefits to this reaction from the presence of the $\mathrm{Pt(PBu^t{}_3)}$ group has been then assessed.

3.1. Bimetallic Paths: The Initial Complex. The reaction cycle for the insertion of phenylacetylene into metal-hydride bonds in bimetallic PtOsSn complexes is presented in Scheme 1. Starting from the initial complex **1**, the coordination of phenylacetylene leads to complex **2** and to the experimentally observed products **3** and **4**.

Several conformations are already possible for the initial complex **1**, as shown in Figure 3. To better identify all these structures, the following nomenclature will be used: the "b" exponent (respectively "nb") means that a carbonyl group is (not) in a bridging position between Pt and Os. The "eq" (equatorial) and "ax" (axial) subscripts will refer to the position of the $\mathrm{SnPh_3}$ group with respect to the plane defined by Pt, Os, and H. In the bridging equatorial cases, CO or H will indicate the substituent is trans to the tin group. The relative energies of these species are also reported Figure 3. It immediately appears that the complexes featuring a bridging carbonyl are the most stable, since these conformations have a formal saturation at both metal atoms. On the contrary, the position of the tin group only slightly affects the energetic order, the differences between axial and equatorial positions being lower than 4 kcal/mol. Even if, in accordance with an intuitive reasoning based on the sterical hindrance of the $\mathrm{SnPh_3}$ group, conformers with equatorial substituent are slightly favored, their stabilization extent is of the same magnitude of the expected error bar of our computational protocol. For this reason, all the three most stable conformations, namely, $\mathbf{1^b_{ax}}$, $\mathbf{1^b_{eqCO}}$, $\mathbf{1^b_{eqH}}$, will be retained in the following. Moreover, dynamical internal conversions from one conformation to another may occur in solution. Indeed, the axial complex has been fully characterized at the experimental level, but low-temperature NMR experiments[17] have shown that these interconversions exist.

3.2. Bimetallic Paths. The products resulting from the phenylacetylene coordination are sketched in Figure 4. The label **2a** denotes products where the phenyl of the phenylacetylene is closer to Os than to Pt, while **2b** indicates the opposite case. It is found that, whatever the alkyne orientation, the phenylacetylene coordination is endothermic, with a significant difference between the two possible isomers (more than 5 kcal/mol). This energy variation is due to the steric repulsion in **2b** between the phenyl of the phenylacetylene moiety and the *tert*-butyl groups carried by the phosphorus atom. Indeed, the shortest distance between these two fragments is about 2.5 Å, while the smallest distance between the phenyl of phenylacetylene and the phenyls carried by the tin atom in **2a** is about 3.6 Å.[35] A proof of the preponderant role of steric hindrance is the fact that the coordination is conversely found stabilizing when a small structural model is considered in which the *tert*-butyl and phenyl groups on phosphorus and on tin are substituted by methyl ones. In this case, **2a** and **2b** are more than 6 kcal/mol stable than the lowest initial complex.

It can also be noticed that the $C_\alpha{-}C_\beta$ bond in phenylacetylene is significantly shortened upon interaction with the metal atom, having a length (1.34 Å for instance in $\mathbf{2a_{eqH}}$ and $\mathbf{2b_{eqH}}$) close to that of a double bond. This suggests that the word "coordination" is more convenient than accurate since already the formation of **2a** or **2b** can be viewed as close to an insertion process. Indeed, in the most stable initial compound ($\mathbf{1^b_{ax}}$), a carbonyl group is in

---

(35) The given values, 2.5 Å, correspond to the distance between a carbon of the phenylacetylene and one of the hydrogens of a *tert*-butyl group, while 3.6 Å refers to the distance between a carbon of the first-mentioned moiety and one of the hydrogen atoms of the phenyl groups on the tin atom.

a bridging position between Pt and Os. When phenylacetylene comes into the metallic coordination sphere, this CO no longer interacts with Os, but it is fully transferred to the Pt atom. A consequence of this mixed situation (between simple coordination and total insertion) is that the distance between Pt and Os increases (from typically 2.9 Å in **1** to 3.0 Å in **2a** and 3.1 Å in **2b**). Another difference between **2a** and **2b** is in the interaction of the bridging-hydrogen atom with the metals, leading to metal–hydrogen distances slightly different in the two cases: Pt–H = 1.70 Å and Os–H = 1.87 Å in $\mathbf{2a_{eqH}}$, Pt–H = 1.67 Å and Os–H = 1.97 Å in $\mathbf{2b_{eqH}}$. The electronic density is, thus, generally less delocalized between the metals in **2b**, and that is also an explanation for the lower stability of these species.

Various insertion products can then derive, depending on which carbon, external C_α or internal C_β, is bound to one of the two metals, Pt or to Os. Furthermore, carbon atoms are involved in σ or π bonds. These products will be accordingly labeled $\boldsymbol{\sigma\pi}$ or $\boldsymbol{\pi\sigma}$, respectively if the interaction is σ with Pt and π with Os, or *viceversa*. Four classes of products can be, therefore, considered: $^{\alpha}\boldsymbol{\sigma\pi}$, $^{\beta}\boldsymbol{\sigma\pi}$, $^{\alpha}\boldsymbol{\pi\sigma}$, $^{\beta}\boldsymbol{\pi\sigma}$, as shown in Figure 5 Of these, only products belonging to the two first two have been experimentally detected, namely, $^{\alpha}\boldsymbol{\sigma\pi}_{\mathbf{eq}}$ or $^{\beta}\boldsymbol{\sigma\pi}_{\mathbf{eq}}$ (**3** and **4** in Scheme 1). It is important to notice that the computed structures of these products are in fair agreement with the X-ray data of reference 17. For instance, the $PtOsC_\alpha C_\beta$ angle is −36.1° in experiments and −35.4° at the theoretical level for $^{\alpha}\boldsymbol{\sigma\pi}_{\mathbf{eq}}$, and the C_α–C_β bond length in $^{\beta}\boldsymbol{\sigma\pi}_{\mathbf{eq}}$ is predicted to be 1.410 Å and 1.405 Å, respectively, in experiments and theory.

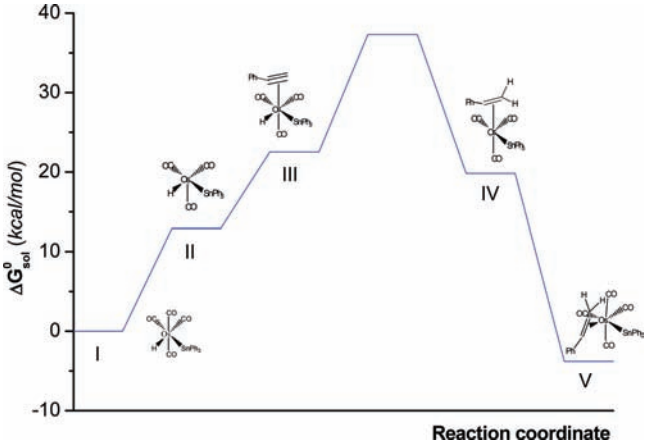

Figure 2. Gibbs free-energy profile for the phenylacetylene insertion with the monometallic catalyst.

Some trends can be drawn regarding the energies of the insertion products. For instance, at a given conformation of the tin group, the $\boldsymbol{\sigma\pi}$ products tend to be more stable than the $\boldsymbol{\pi\sigma}$ ones: $^{\alpha}\boldsymbol{\sigma\pi}_{\mathbf{ax}}$ is, for instance, 3.2 kcal/mol lower in energy than $^{\alpha}\boldsymbol{\pi\sigma}_{\mathbf{ax}}$, while the energy difference between, $^{\beta}\boldsymbol{\pi\sigma}_{\mathbf{eq}}$ and $^{\beta}\boldsymbol{\sigma\pi}_{\mathbf{eq}}$ is only 1.3 kcal/mol. Moreover species with the carbon β involved in the σ bond to the metal (as $^{\beta}\boldsymbol{\sigma\pi}$ or $^{\beta}\boldsymbol{\pi\sigma}$) are more stable than the corresponsing α species because of the reduced steric interaction between the phenyl of phenylacetylene and the $SnPh_3$ moiety (see Figure 4).

More in general, the three most stable products are of $\boldsymbol{\sigma\pi}$ type ($^{\beta}\boldsymbol{\sigma\pi}_{\mathbf{eqPh}}$, $^{\beta}\boldsymbol{\sigma\pi}_{\mathbf{eq}}$, and $^{\beta}\boldsymbol{\sigma\pi}_{\mathbf{ax}}$) products, all being significantly more stable than the reactants (between −13.8 and −11.7 kcal/mol). This finding is in agreement with the experimental evidence that no $\boldsymbol{\pi\sigma}$ have been observed. However, one $\boldsymbol{\pi\sigma}$ species, namely, $^{\beta}\boldsymbol{\pi\sigma}_{\mathbf{eq}}$, is practically isoenergetic with the $^{\beta}\boldsymbol{\sigma\pi}_{\mathbf{ax}}$ (−11.6 vs −11.7 kcal/mol) product. To better investigate the formation kinetics of all these products, all the transition states leading to the discussed insertion products have been characterized, and their energies are collected in Figure 6. From these values it immediately appears that $\boldsymbol{\pi\sigma}$ products are kinetically favored, since $\mathbf{TS}_{\pi\sigma}^{\alpha,\mathrm{eq}}$, $\mathbf{TS}_{\pi\sigma}^{\beta,\mathrm{eq}}$, and $\mathbf{TS}_{\pi\sigma}^{\alpha,\mathrm{eqPh}}$ have an energy lower than 36 kcal/mol where all $\mathbf{TS}_{\sigma\pi}$ are higher than 40 kcal/mol. It results,

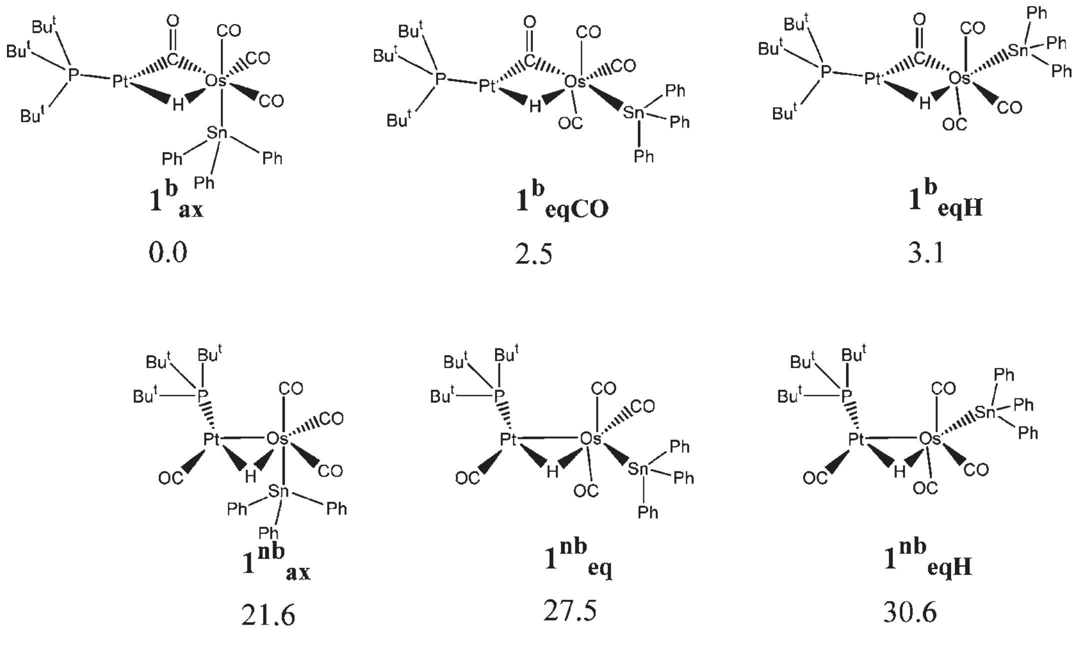

Figure 3. Sketches and relative Gibbs free-energies (kcal/mol) for the initial complexes **1**.

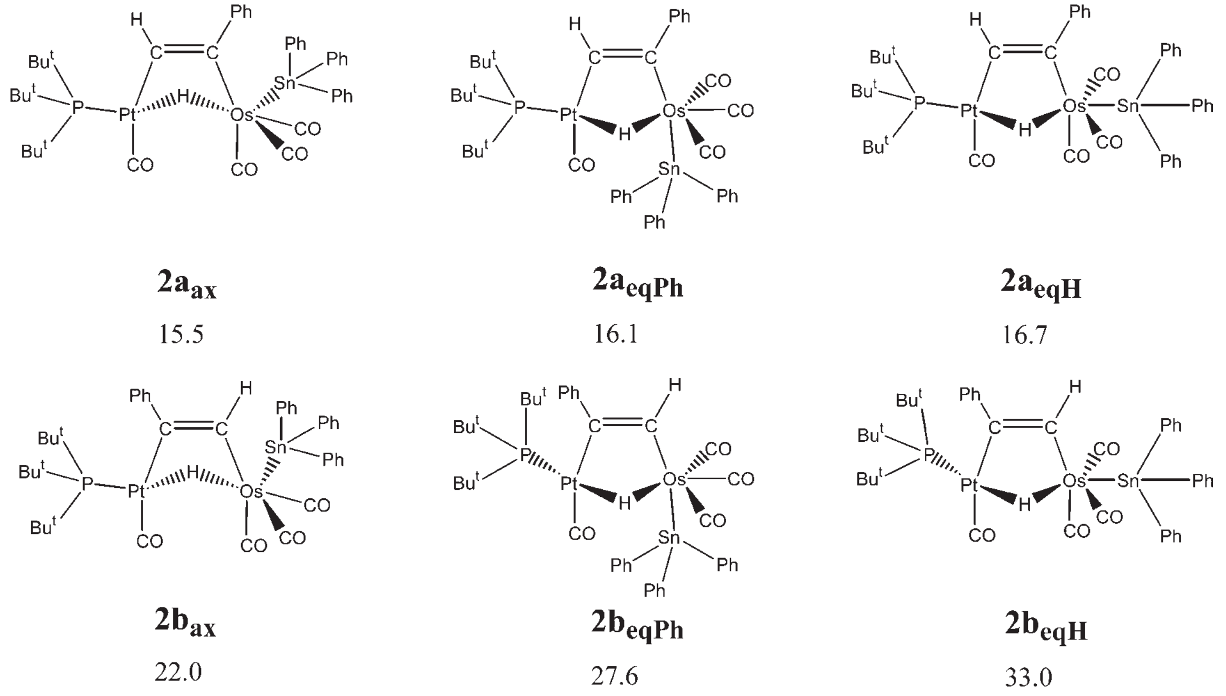

$2a_{ax}$ 15.5

$2a_{eqPh}$ 16.1

$2a_{eqH}$ 16.7

$2b_{ax}$ 22.0

$2b_{eqPh}$ 27.6

$2b_{eqH}$ 33.0

Figure 4. Sketches and relative Gibbs free-energies (kcal/mol) for the possible coordination complexes. The energy zero corresponds to the most stable initial complex (**1^{b}_{ax}**, see Figure 2) and phenylacetylene.

from these data, that the $\pi\sigma$ products are kinetically favored.

It is interesting to notice that there are clear differences between isomers: for instance, the Gibbs energy difference between **$TS^{\alpha,eq}_{\pi\sigma}$** and **$2a_{eqH}$** is equal to 13.5 kcal/mol, whereas the one between **$TS^{\beta,eq}_{\pi\sigma}$** and **$2b_{eqH}$** equals 8.6 kcal/mol. Similarly, these barriers are 19.5 kcal/mol from **$2a_{eqPh}$** to **$TS^{\alpha,eqPh}_{\pi\sigma}$** and 13.7 kcal/mol between **$2b_{eqPh}$** and **$TS^{\alpha,eqPh}_{\pi\sigma}$**. This feature can be easily explained from the geometric data already reported. Indeed, the transferred hydrogen is closer to Pt in **2b** than in **2a**. As the H-acceptor in **2b** is also located near Pt, it follows that the distance that the hydrogen atom must cover is smaller in **2b** than in **2a**, and, following the Hammett principle, the corresponding activation barrier for this step is lower. However, the overall activation energy ΔG°_{act} is the sum of the coordination and insertion energies, and it is similar (30.2 and 30.6 kcal/mol) for the formation of ${}^{\alpha}\pi\sigma_{eq}$ and ${}^{\beta}\pi\sigma_{eq}$, thus suggesting that both products are likely to be formed. Moreover, all of these processes are hardly reversible since the barriers for the regeneration of the metal-hydride complexes require more than about 40 or 50 kcal/mol.

It must be noted that terminal alkynes are known to be susceptible to isomerization into vinylidenes in the presence of transition metal complexes.[36,37] This possibility has been also investigated, but no stable species were identified.

In summary, the previous theoretical data well elucidate the multistep reaction allowing the formation of the two experimentally observed $\sigma\pi$ products $PtOs(CO)_4(SnPh_3)(PBu^t_3)[\mu\text{-}HCC(H)Ph]$ and $PtOs(CO)_4(SnPh_3)(PBu^t_3)[\mu\text{-}C(Ph)CH_2]$ (3 and 4 in Scheme 1).[17] However, this theoretical analysis suggests that also a $\pi\sigma$ product could be observed. So, to explain such a discrepancy, the $\pi\sigma \to \sigma\pi$ isomerization has been also investigated, by considering four isomerization paths, namely, ${}^{\alpha}\pi\sigma_{eq} \to {}^{\alpha}\sigma\pi_{eq}$, ${}^{\beta}\pi\sigma_{eq} \to {}^{\beta}\sigma\pi_{eq}$, ${}^{\alpha}\pi\sigma_{eq} \to {}^{\beta}\sigma\pi_{eq}$, and ${}^{\beta}\pi\sigma_{eq} \to {}^{\alpha}\sigma\pi_{eq}$. Their energies are collected in Figure 7. The first two reactions are energetically accessible and consist in the transfer of the phenylacetylene moiety from Pt to Os. The corresponding transition states are characterized by the position of the β-carbon (previously bound to Pt) in an equidistant position between Pt and Os atoms. The associated activation barriers are relatively low (16.7 and 10.4 kcal/mol) if compared with the other TS energies of the reaction path. It must be noticed that in this case, a valuable energetic difference exists between both paths, **TS^{β}_{eq}** being favored. A simple qualitative argument, based on steric hindrance, can account for this fact: in **TS^{α}_{eq}**, the $C_{\alpha}H_2$ moiety remains in the vicinity of Pt and Os, whereas in **TS^{β}_{eq}** the entire phenyacetylene moiety (except the external carbon that is involved in the process) is outside of the coordination sphere of the transition metals. Another important point is that these barriers are smaller than the ones for insertion, so that such transformations are likely to occur once the $\pi\sigma$ products are formed.

The two other isomerization paths, ${}^{\alpha}\pi\sigma_{eq} \to {}^{\beta}\sigma\pi_{eq}$ and ${}^{\beta}\pi\sigma_{eq} \to {}^{\alpha}\sigma\pi_{eq}$, involve the exchange of the coordinated carbon. Accordingly, these processes involve two simultaneous events: a hydrogen shift from the carbon to which it was transferred to the other one and the transfer of the phenylacetylene moiety from Pt and Os. This complex transformation accounts for the calculated prohibitive activation barriers (more than 40 kcal/mol, see Figure 7).

In conclusion, the reaction mechanism at the bimetallic center, leading to the formation of the $\sigma\pi$ products, consists in the phenylacetylene coordination, an endothermic

---

[36] (a) Oliván, M.; Clot, E.; Eisenstein, O.; Cauton, K. G. *Organometallics* **1998**, *17*, 3091. (b) Oliván, M.; Clot, E.; Eisenstein, O.; Cauton, K. G. *Organometallics* **1998**, *17*, 897.

[37] Bustelo, E.; Carbó, J. J.; Lledós, A.; Mereiter, K.; Puerta, M. C.; Valerga, P. *J. Am. Chem. Soc.* **2003**, *125*, 3311.

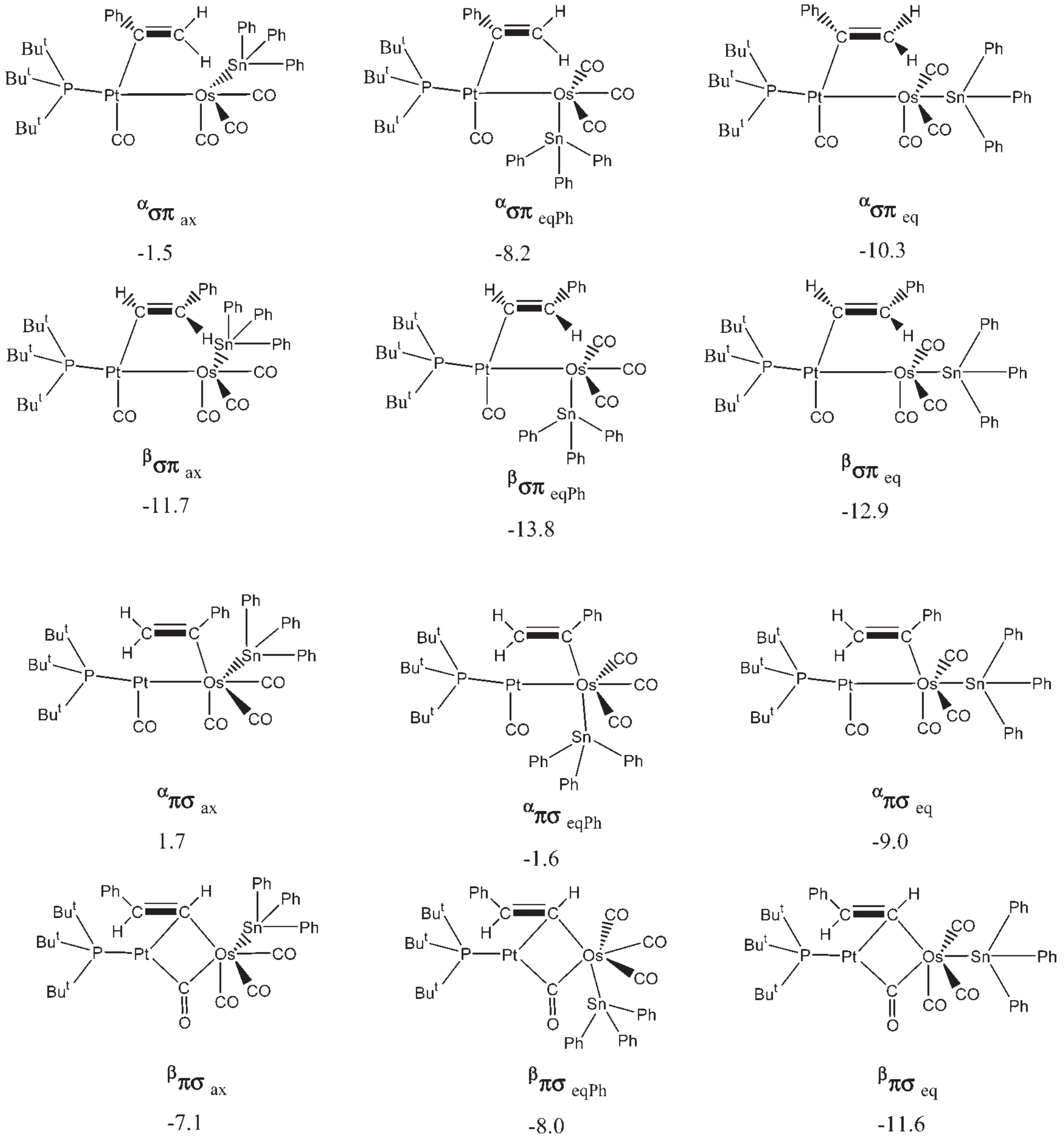

$^{\alpha}\sigma\pi_{\text{ax}}$ -1.5 | $^{\alpha}\sigma\pi_{\text{eqPh}}$ -8.2 | $^{\alpha}\sigma\pi_{\text{eq}}$ -10.3

$^{\beta}\sigma\pi_{\text{ax}}$ -11.7 | $^{\beta}\sigma\pi_{\text{eqPh}}$ -13.8 | $^{\beta}\sigma\pi_{\text{eq}}$ -12.9

$^{\alpha}\pi\sigma_{\text{ax}}$ 1.7 | $^{\alpha}\pi\sigma_{\text{eqPh}}$ -1.6 | $^{\alpha}\pi\sigma_{\text{eq}}$ -9.0

$^{\beta}\pi\sigma_{\text{ax}}$ -7.1 | $^{\beta}\pi\sigma_{\text{eqPh}}$ -8.0 | $^{\beta}\pi\sigma_{\text{eq}}$ -11.6

Figure 5. Sketches and relative Gibbs free-energies (kcal/mol) for the insertion products. The energy zero corresponds to the most stable initial complex ($\mathbf{1}^{\mathbf{b}}_{\mathbf{ax}}$, see Figure 2) and phenylacetylene.

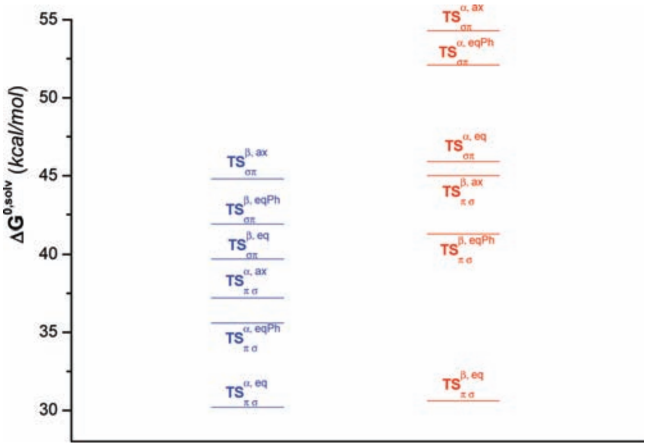

Figure 6. Relative Gibbs free-energy (kcal/mol) for the transition states for the insertion process. The energy zero corresponds to the most stable initial complex ($\mathbf{1}^{\mathbf{b}}_{\mathbf{ax}}$, see Figure 2) and phenylacetylene.

reaction requiring at least about 16 kcal/mol, followed by the insertion into the metal-hydride bond, which is characterized by a barrier of about 14 kcal/mol. Eventually, minor $\pi\sigma$ products can then isomerize to the corresponding $\sigma\pi$ species following a path requiring 10 kcal/mol. The identified reaction path is, therefore, characterized by non-prohibitive reaction free energies and well supported by the agreement with the experimental data.

3.3. Mono- vs Bimetallic Reaction Paths. To have a direct comparison of the two mechanisms, the overall energy profiles are reported in Figure 8. The most striking feature concerns the differences in energy of the two rate determining steps (30 and 37 kcal/mol for the bi and mono metallic path, respectively) and the thermodynamic stabilization of the products (**V** and $^{\alpha}\pi\sigma_{\text{eq}}$, -5 and -9 kcal, respectively). Therefore, the addition of a second transition metal already has a significant effect on the

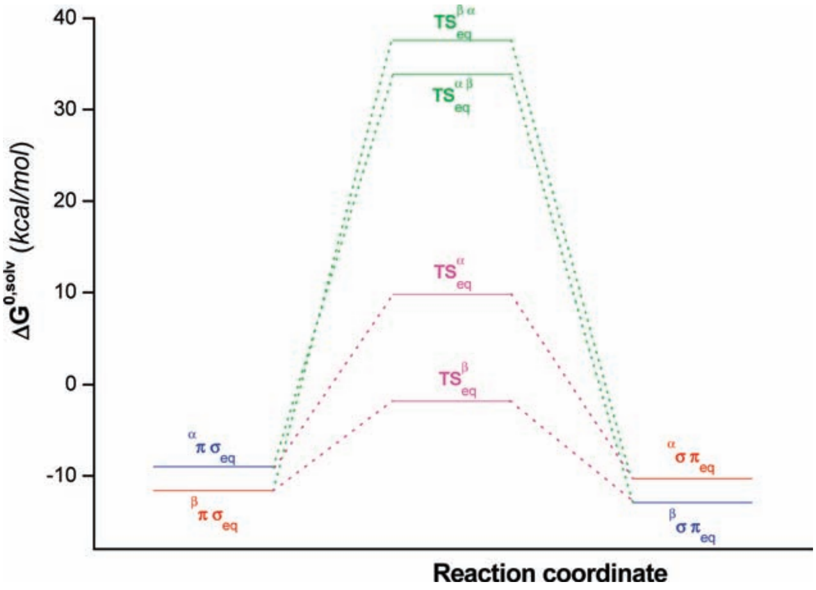

Figure 7. Gibbs free-energy profiles for $\pi\sigma \rightarrow \sigma\pi$ isomerizations. The energy zero corresponds to the most stable initial complex ($\mathbf{1}^{b}_{ax}$, see Figure 2) and phenylacetylene.

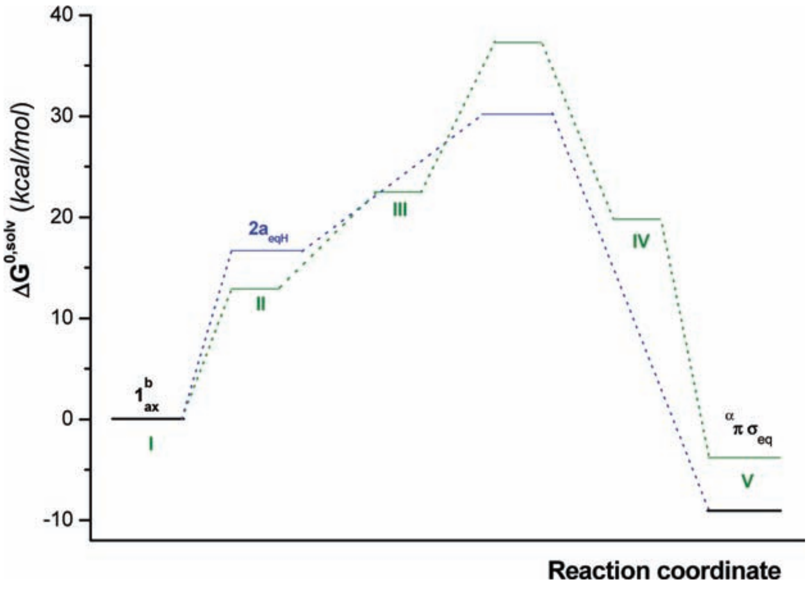

Figure 8. Plot of the Gibbs free-energy profile for the monometallic (green) and bimetallic (blue) reactions. Please note that the reaction coordinate is not the same for the two paths.

overall energetic balance, leading to a more favorable kinetics and thermodynamics of the reaction.

The obtained results, however, indicate that another important beneficial effect of the second metal atom is in the release of CO from the Os center, Pt being a rather good CO acceptor. Indeed the CO and the following phenylacetylene coordination require 13 and 23 kcal/mol in the monometallic catalyst (**II** and **III** in Figure 8), while the two concerted steps demand only 17 kcal/mol in the bimetallic species. More important CO never leaves the metals coordination sphere, but is just shifted from one metal to the other (from Os to Pt). This is, of course, not possible in the monometallic center where the CO leaves the coordination sphere of Os and its recoordination, under entropic and diffusion control, is needed to generate a thermodynamically stable product (from IV to V, see Figure 8). In other words, the role of the second metal is to significantly decrease the energy required for the CO release to create a vacant site at the metallic center through its coordination to a close metallic acceptor (Pt).

The second metal does not have a relevant effect on the insertion process which, whatever the case, is not the most energetically demanding step, requiring an activation of about 15 kcal/mol. However, the Pt group is sterically hindered and thus makes the phenylacetylene coordination more difficult. As the efficiency of the complex depends both on the CO releasing and on the alkyne coordination facilities, one can understand that the role of the benefit of the second metal is not easy to understand, a balance having to be found between these two antagonist effects.

4. Conclusions

In this paper, a detailed theoretical investigation is given of the phenylacetylene insertion in metal-hydride bonds of a bimetallic (Os, Pt) catalyst. The identified reaction path consists in the phenylacetylene coordination followed by the insertion into the metal-hydride bond, and it leads to the formation of the experimentally observed products. Both steps do not require large energies incompatible with the experimental conditions. Higher energy products, minor species not conforming to the experimental findings, could easily isomerize to the experimental molecules. Furthermore, some insights on the cooperative effects due to the presence of the second metal (here Pt) have been given by a comparative analysis with the reaction mechanism involving the monometallic (Pt) catalyst. The obtained theoretical results suggest that the second metal acts as acceptor in the CO release, required to create a vacant site at the metallic center for the incoming phenylacetylene, leading to a significant decrease of the reaction energies. At the same time the second metal does not have a relevant effect on the insertion process which always requires a low activation energy.

Acknowledgment. V.T. thanks the Department of Chemistry, University of Calabria for the warm hospitality.

Supporting Information Available: Further details on alternative paths for the monometallic and bimetallic catalysts, the computational protocol, references, views of the ONIOM optimized geometries and main geometric parameters, and Cartesian coordinates of the ONIOM optimized structures, three lowest harmonic vibrational frequencies, and thermochemistry. This material is available free of charge via the Internet at http://pubs.acs.org.